sciendo
DOI: 10.2478/agriceng-2022-0009
ISSN 2083-1587; e-ISSN 2449-5999
2022,Vol. 26,No.1, pp.105-117
Agricultural Engineering
www.wir.ptir.org

REVERSE ENGINEERING IN MODELING AGRICULTURAL PRODUCTS

Marek Boryga[a], Paweł Kołodziej[a*]

[a] Department of Mechanical Engineering and Automation, University of Life Sciences in Lublin, Poland, marek.boryga@up.lublin.pl, ORCID 0000-0002-5991-7871; pawel.kolodziej@up.lublin.pl, ORCID 0000-0003-0479-1770

* *Corresponding author: e-mail: pawel.kolodziej@up.lublin.pl*

ARTICLE INFO

Article history:
Received: May 2022
Received in the revised form:
May 2022
Accepted: June 2022

Keywords:
reverse engineering,
3D scan,
interpolation spline,
projection of sugar beet root geometry

ABSTRACT

The purpose of the study was to use reverse engineering to model biological products, especially sugar beet root. In the process of creating the solid model, the appropriate tools available in the 3D design environment were applied. The 3D scan of the beet, in the form of a spatial point cloud, was used to project the root geometry. This was, in turn, used to construct a triangulation grid that includes nodal points of triangles. The subsequent steps presented the process of creating a solid model using the Interpolation Spline tool. Attention has been paid to the possibility of modifying the geometry by inserting additional points into the existing interpolation spline and changing angular position as well as the distance of the structural planes. Geometry mapping error values were determined with regard to the reference model depending on the spread value of the Structural Planes. Error courses are non-linear with a logarithmic line trend (surface field error) and a linear line trend (volume error). The effects demonstrated the usefulness of geometry projection and its applicability to support the strength testing of biological materials, with particular emphasis on dynamic tests using whole roots.

Introduction

Reverse engineering is a process of examining real objects to create documentation in the form of a 2D or 3D model. This process had been applied in many industrial sectors even before the introduction of modern digital support techniques. Initially, a detailed performance documentation of the object was created using data obtained with conventional measuring instruments. The emergence of coordinate measuring technology followed by 3D scanning techniques enabled the collection of a large number of spatially distributed points allowing the reconstruction of the shape of the object with a certain degree of precision. 3D scanning is the most characteristic step in reverse engineering and therefore is often associated with it. Measurement of the shape of real objects with 3D scanners and computer modeling to obtain a virtual spatial model is used in many fields of science and technology:

- mechanics and mechanical engineering,
- manufacturing technology,
- metrology and quality control,

– design,
– ergonomics and anthropology,
– life sciences,
– medicine and dentistry,
– archeology, museum management, art,
– architecture,
– advertising, film, TV, computer games and 3D animation.

Figure 1 shows the idea of reverse engineering for a typical mechanical engineering application.

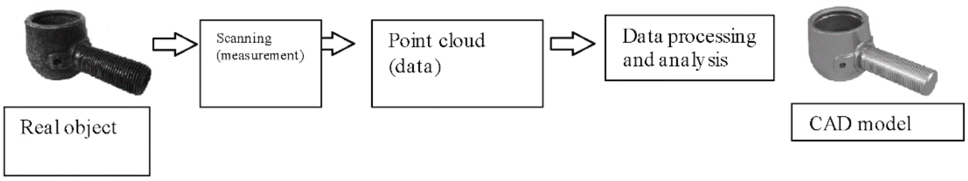

Figure 1. The concept of reverse engineering in machine construction

Reverse engineering is a broadly discussed area of scientific work. Sokovic and Kopac (2006) presented the applicability and benefits of reverse engineering methods and techniques in the manufacturing process, especially for parts without 3D-CAD documentation. They report that applying reverse engineering methods is absolutely necessary as it allows reproducing and digitalizing the geometry of the surface of the product for further use in CAD/CAE/CAM systems. Ye et al. (2008) proposed an innovative design method called Reverse Innovative Design (RID). The RID method facilitates the initial design and subsequent use of its results by means of digital 3D design applications. The foundation of RID is to define and construct parametric solid models based on features derived from scanned data. Wang et al. (2012) developed a method of creating 3D models using an edge-based surface mesh of the part. They used the divide-and-conquer strategy to create the shapes of all the part primitives and then used solid merging and surface trimming to assemble the primitives into a final 3D model. They tested several industrial parts to illustrate the effectiveness and reliability of the proposed approach. Based on the measurement results and the digitization process, Dubravcik and Kender (2012) made a 3D model of a damaged cog. This model became a source for further measurements and printing of a new cog on a 3D printer. The new cog was successfully used as a replacement for the original damaged element. The authors found that digitalizing the new cog and overlaying the original and the new point clouds allowed verifying the differences and forming the final shape of the 3D model of the cog. Kovacs et al. (2015) reported that creating digital models is an important area of reverse engineering. The noise and numerical nature of the algorithms (point cloud alignment, mesh processing, segmentation, and surface matching) cause inaccuracies such as lack of parallelism or perpendicularity, poor roundness, concentric holes, axis skews, etc. The authors presented algorithms to eliminate these inaccuracies and create "perfect" models suitable for further CAD/CAM applications. Based on the example of a two-section master cylinder body, Bochnia (2019) discussed the procedure of building a surface model and dimension inspection using data obtained from a 3D scanner. The author pointed out that there is no simple transition from a surface model to a solid CAD model, which demonstrates a large untapped potential for reverse engineering.

Some of the research works discuss the evaluation of the measurement capabilities and accuracy of solid model reproduction. Gapinski et al. (2014) presented the results of a comparative study conducted using a coordinate measuring machine, an optical scanner and a metrological CT scanner. The differences in results for the techniques presented did not exceed 0.05 mm. The authors determined that the touch-sensitive measurement creates an information gap between data points. The optical scanner is impractical for collecting point data in small-diameter holes, and the CT scanner has the disadvantage of creating artifacts. Vagovsky et al. (2015) evaluated the measurement capabilities of the 3D GOM ATOS Triple Scan II using statistical methods. Ameen et al. (2018) compared two portable systems using laser scanning and optical scanning by applying white light for automotive applications. The scanners were compared in terms of accuracy, scanning time, number of triangles in the *.stl file, ease of use, and handiness. The results showed that the laser scanner was better than the white-light scanner in terms of accuracy, while the white-light scanner was better in terms of acquisition speed and number of triangles. Burek et al. (2019) analyzed the precision of creating a solid model based on surfaces generated for different tolerance values of triangles. Reconstruction engineering methods were used to develop the digital model. Pieróg et al. (2020) described the process of copying bas reliefs. These sacral culture objects were scanned using an industrial 3D scanner and copied using a five-axis milling unit. Rescanning showed that the distance between the surface obtained and the theoretical surface of the object does not exceed 0.5 mm. Sikorski et al. (2016) presented the use of the reverse engineering method to model a personalized hip endoprosthesis. The final effect of the scanning process was a 3D model of a pelvis. The ability to size the pelvic hip acetabular bore provided the data necessary to design a custom hip endoprosthesis.

Since most agricultural products are irregular in shape, their physical and engineering analysis is very complicated. Therefore, there is little work on this subject area. Costa et al. (2011) stated that among the factors governing the sales of agricultural products, their appearance and, in particular, their shape play a key role. The authors proposed a new automated shape analysis system that can be useful for both scientific and industrial purposes. Celik et al. (2017) used reverse engineering methods to accurately describe geometric features (size, shape, volume, etc.) of pecan nuts. The data obtained during the scanning were processed by the authors using scanner software. Then, a 3D model was created in a solid modeling application, SolidWorks. After constructing 3D solid models, the authors made precise measurements of geometric features and conducted comparative rheological studies using the finite element method. They concluded that the data on the behaviour of nuts during deformation could be used in the design of components for agricultural machinery and food processing machinery.

In conclusion, please note that in the case of biological products, analyzing morphological properties (species characteristics, varietal characteristics, etc.) requires methods for mapping the geometry of irregular solids (e.g. fruits, roots, seeds), as well as rheological studies using the finite element method (FEM). Improving the description of individual shapes of agricultural products also results from the need to determine the positions inside machines (e.g. cleaners) or the effects of static or dynamic interactions with its elements.

The aim of this work was to model sugar beet root using the appropriate 3D design tools. A 3D scan of the beet root, which is a spatial point cloud, was used to help map the root geometry. The cloud was then used to construct a triangulation grid that included triangle nodal points. The created mesh was subjected to digital closing and smoothing, to obtain a closed surface, called the watertight model. Further digital processing yielded the final result in the form of a 3D model.

Material and Methods

Prior to the scanning process, a spatial object was prepared, i.e., a sugar beet root cleaned from the soil stuck to the surface, which was placed vertically on a stand allowing free 360° access to the root. Scanning was performed with the EinScan Pro HD 3D scanner developed by Shining 3D Tech Co. Ltd. (China). The scanner software allowed scanning with a turntable or manually. The accuracy then ranges from 0.1 mm for fast manual scans to 0.04 mm for stationary scans using the turntable as part of the scanning kit. Since the beet root has an irregular shape and surface with variable curvature radii, it was scanned using a turntable. The root was placed on a table with a stand, and the option Fixed Scan with Turntable was selected. Scanning any part of a solid requires specifying an angle that covers the selected part of the object outline and dividing this angle into an appropriate number of single scans, to later reconstruct the view of the studied surface. To represent the root shape as a solid with as much detail as possible, 360° scanning was divided into 32 scans. During scanning, the table rotates at a programmed speed and stops at 11.25° intervals while the scanner creates a model of the selected surface using white light. Therefore, light with limited brightness should be used in the process. The included software enables registering individual scans, creating a spatial image consisting of individual points in the form of a cloud, and constructing a triangulation grid (mesh grid). Based on the grid, the so-called waterproof model is constructed, which is a representation of the examined surface. Figure 2 shows the digital beet root model in the form of a point cloud (Figure 2a) and a triangular grid (Figure 2b). The magnification shown in Figure 2b was obtained using Inventor software.

a) *b)*

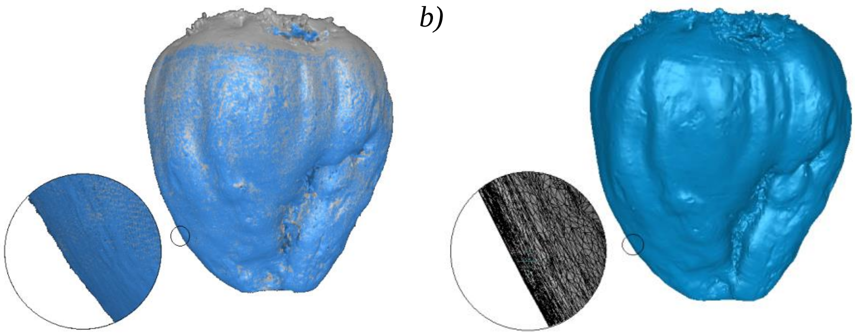

Figure 2. Figure 2. Digital model of a beet root in the form of: (a) cloud points, (b) triangular grid

A CAD-editable file was created using the free MeshLab software and then uploaded to the Inventor software. In the first step, a construction plane was created adjacent to the beet tailing surface (Fig. 3a). Then a sketch was created as an outline of the tailing surface (Fig. 3b). The Interpolation Spline tool was used to create the sketch. The first point on the visible edge of the section was selected and then subsequent matching points were created. To close the loop, the last point was created to match the starting point, and the Close Loop option was selected. In the next step, a new construction plane was created – parallel to the first one, at a distance of dimension *d*. Another sketch was created in this plane, which uses the shape of the outer edge of the cross section to form the next outline of the outer edge of the beet root (Fig. 3c). Finally, the sketches were used to make the first layer of the model of the beet root's solid. The Composite extrusion tool (Figure 3d) was used to create the layer.

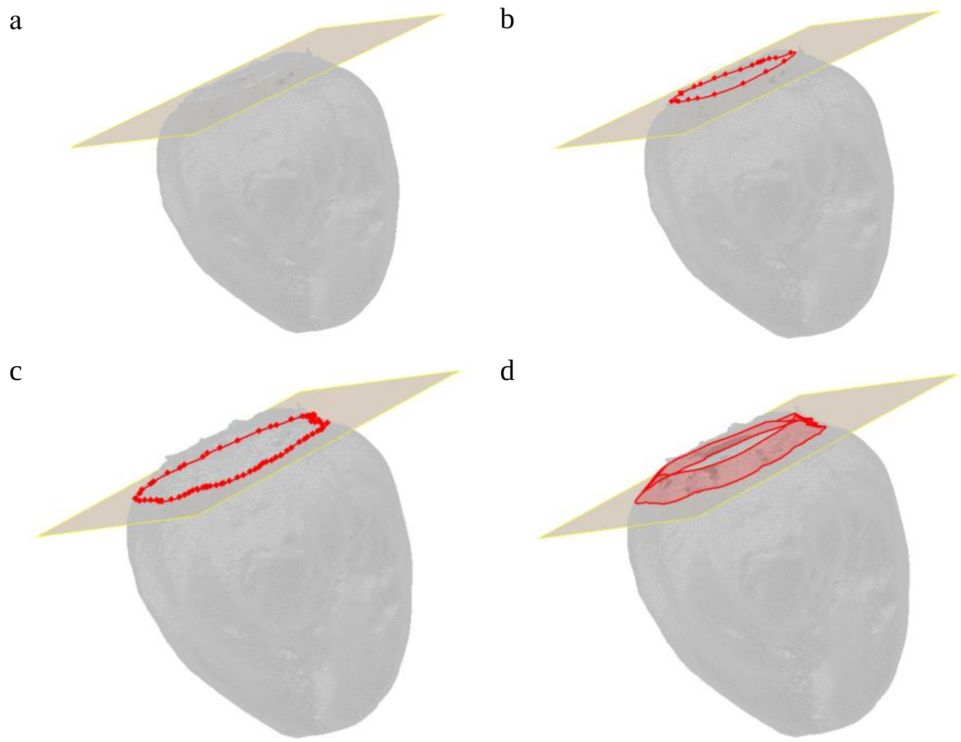

Figure 3. The creation of a 3D model of the beet root: a) initial construction plane, b) outline sketch of the tailing surface, c) outline sketch of the cross-section in the second construction plane, d) first composite extrusion.

Figure 4 shows an example of the outline of one of the cross sections of the beet. As mentioned above, the outline was created using the Interpolation Spline tool. After the initial introduction of points, it is possible to edit the resulting shape by:

– dragging the points to reposition them,
– inserting an additional point anywhere on the created shape using the Insert Point command,
– adjusting the spline shape using the Activate Handle command that activates the tangent handles for a selected point.

In the detail shown in Figure 4, the yellow color indicates the curvature of the spline at the selected point, while the red color indicates the tangent with the activated handles.

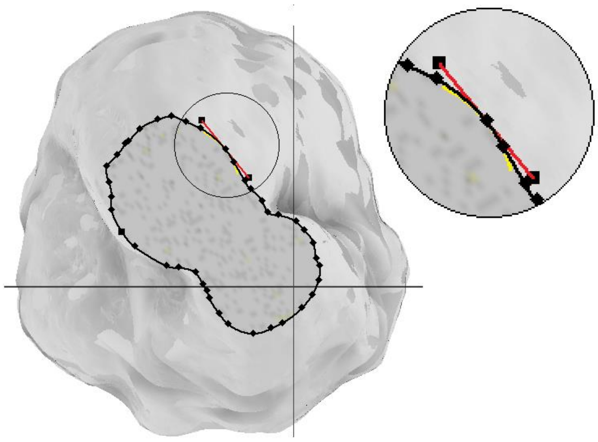

Figure 4. A closed outline of a sample cross-section delimiting a beet root cross-section with the activated handle of a selected point.

An important step in the algorithm is the selection of the distance *d* between successive planes in which the sections' outline sketches are created. For the analyzed beet root, which was 160 mm long, *d* values of 25, 20, 15, 10 and 5 mm were applied. The presented algorithm assumes a fixed distance *d*, but a variable distance *d* can be used for fragments of objects with minor or major changes in the shape of adjacent sections.

Figure 5 shows a block diagram of the behavior algorithm that can be used to create solid models of irregularly shaped objects in 3D modeling software.

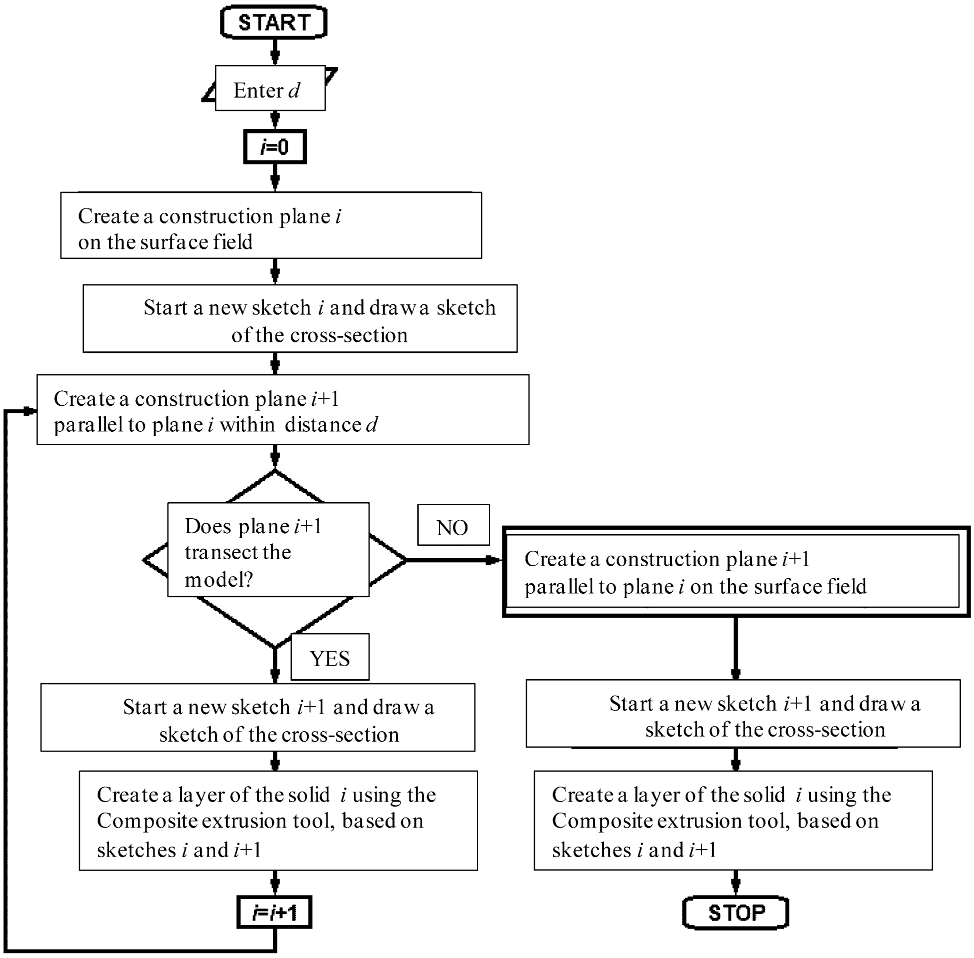

Figure 5. A block diagram of the algorithm for creating a CAD model of irregularly shaped objects

To verify how distance *d* affects the change in geometric parameters, the digital models of the beet root were created for five distances *d*: 25, 20, 15, 10, and 5 mm, while their surface area and volume were compared with the reference model in the form of a triangular grid. The surface area of the reference model was S=70866.797 mm^2 and the volume V=1394828.375 mm^3.

Results and Discussion

Figure 6 shows the digital model of a beet root created with a *d* of 10 mm.

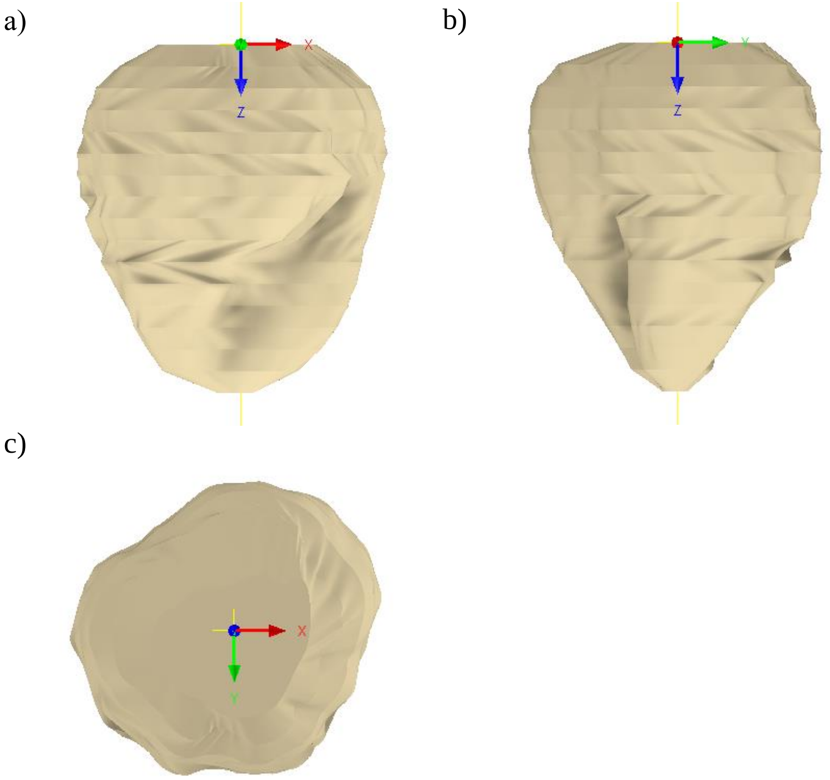

Figure 6. Solid model of a beet root in rectangular projections (d=10 mm): a) main projection, b) side projection, c) top view

A summary of the geometric parameters of the solid models for the adopted values of *d* with respect to the reference model is presented in Tab. 1. As expected, decreasing the value of distance *d* decreases the relative errors calculated for both the area and the volume.

The courses of errors that occur during geometry modeling and resulting from changes in the distance between structural planes are shown in Figures 7 and 8. The courses were supplemented with trend lines and R^2 determination coefficients that are decisive in adjusting the statistical model. It is described with the error change curve, depending on the adopted distribution of the construction planes.

Table 1.
Summary of the geometric parameters of the solid models for the adopted values of d with respect to the reference model.

Translation function *d* (mm)	Area S (mm^2)	Relative error of area δ_S (%)	Volume V (mm^3)	Relative error of volume δ_V (%)
25	64465.778	9.03	1314765.024	5.74
20	65004.092	8.27	1340192.434	3.92
15	65826.323	7.11	1349384.486	3.26
10	67295.988	5.04	1365940.233	2.07
5	70248.940	0.87	1372045.231	1.63

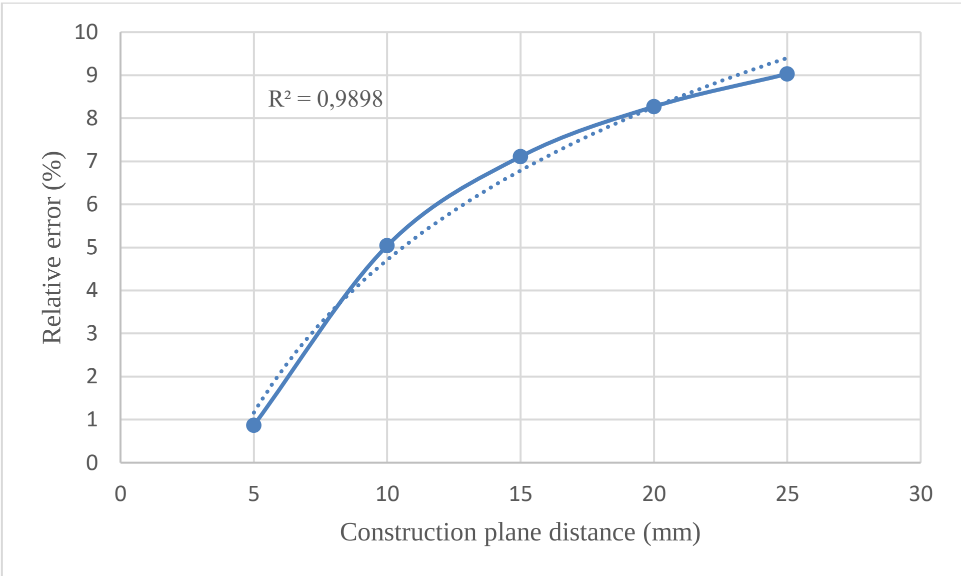

Figure 7. A graph of relative errors of the surface area δ_S depending on the distribution of construction planes during solid modeling.

As mentioned above, 3D solid models of biological products can be used not only for precise description of geometric features (size, shape, volume, etc.) but also for comparative rheological studies using, e.g. FEM.

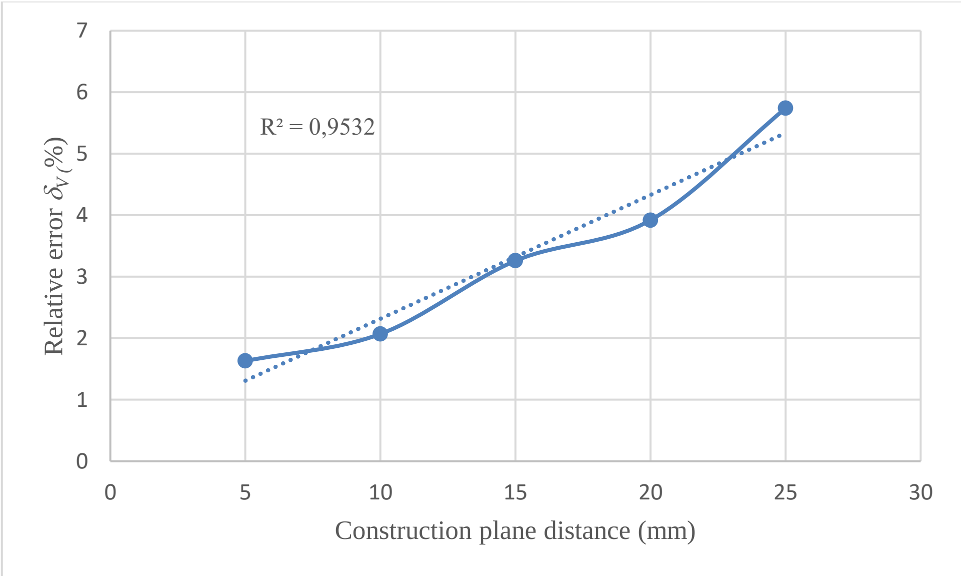

Figure 8. Graph of relative errors of the volume of the solid δ_V depending on the distribution of construction planes during solid modeling.

In modeling biological products, cross sections can also be created in planes located parallel to the longitudinal axis. In the case of the beet root, this way can be used for modeling the contact of the beet with the contact surfaces of the thrust components of machinery and equipment mechanisms, e.g., toppers, lifters, cleaning mechanisms, etc. In such a case, it could be important to define the shape and dimensions of the deformation volume of the beet root during modeling of, for example, mechanical impacts. The use of modeling effects supported by actual beet root shape scans can significantly improve the accuracy of impact test results.

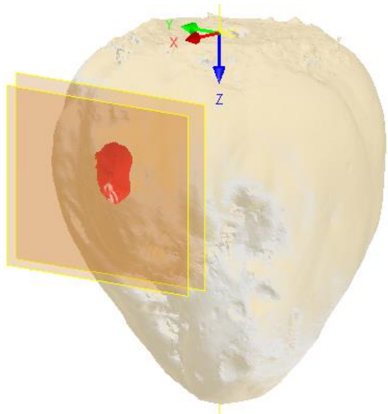

Figure 9. A view of the beet root model with planes parallel to the vertical axis of the roots

Figure 9 shows a view of the beet model with the created planes parallel to the root axis. One of the planes is tangent to the surface, and the other plane is the longitudinal section. The section can be performed at any distance from the extreme point of the surface, also in a distance corresponding to the maximum deformation obtained, e.g. under measurement test conditions. The curvature model of the selected part can then facilitate and speed up the determination of the geometric parameters of the profile (e.g. section surface area or volume of the deformed part) necessary for the performance of stress or statistical analyses. In addition, it can also be used to assess the possibilities of approximating the curves by means of regular solids, e.g. a fragment of a triaxial ellipsoid, the characteristic dimensions of which are shown in Figure 10b.

a) b)

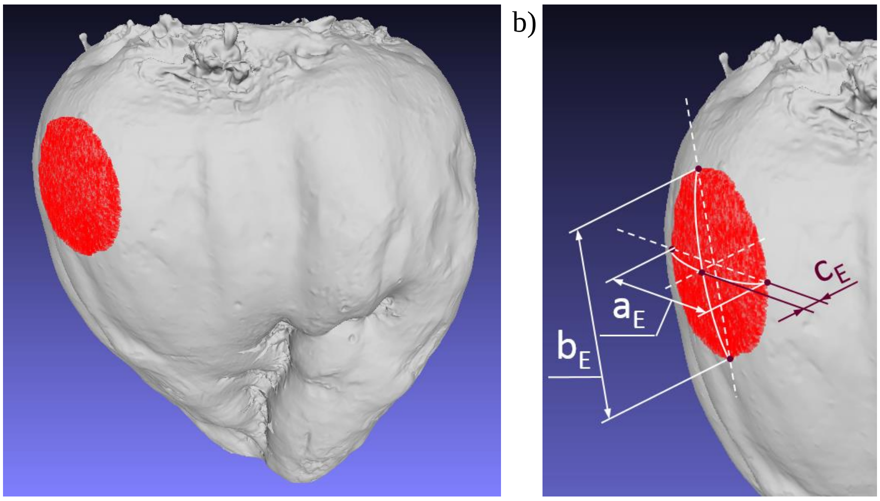

Figure 10. The contact surface of the root with the supporting plane (during e.g. mechanical impact) representing the modeled beet root area: a) position on the beet root model, b) an example of approximation using a segment of a triaxial ellipsoid.

Conclusions

The solid modeling method presented in this paper shows the possibilities of preparing a representation of a sugar beet root using successively introduced constructional planes, whose position in relation to the modeled root simplified the creation of closed solid outlines. At the stages shown, the geometry was reproduced using horizontal (cross-sectional) sections due to the longitudinal shape of the beet bounded from above by the topping surface and from below by the plane of the technological cut after the beet root end is broken off during harvesting.

However, this is not the only way to reproduce geometry. Structural planes can be positioned anywhere to allow the formation of interpolation splines that are necessary to achieve the most accurate geometry of the modeled solid.

Please note also that selected portions of the root geometry can be recreated (Figures 6 and 9) and modeled by changing the angular position (from horizontal to vertical) of the structural planes.

The 3D scans of the root portion produced at that time can be used to dimensionally identify local deformations that are difficult to reproduce with shape standards and measuring tools due to the unique outline of the surface. The result of the above mentioned actions is a block diagram of the 3D CAD model design algorithm (shown in Figure 5), which concludes the process of creating solids with irregular and complex shapes using 3D modeling software.

The relative errors of the beet root geometry modeling with respect to the reference model are presented in Table 1, as well as in Figures 7 and 8. In Figure 7, the course of the surface error δ_S is nonlinear with a logarithmic trend line and a coefficient of R^2 = 0.9898. On the other hand, the course of volume error δ_V increases along a linear trend line and its coefficient of determination is R^2 = 0.9532 (Fig. 8). If the determining factor of the accuracy of the shape;s representation is the 5% error value, then in the case of surface modeling, the distance between construction planes should be set in the range of 5÷10 mm. Assuming the same evaluation criterion for the volume error, the above-mentioned distance between planes can be selected in the range from 5 mm even to approximately 23 mm.

References

Ameen, W., Al-Ahmari, A.M., Mian, S.H. (2018). Evaluation of handheld scanners for automotive applications. *Applied Sciences*, *8*(2), 217.

Bochnia, J. (2019). The use of 3D scanning in reverse engineering. *Mechanik*, 3/2019, 194-196.

Burek, J., Jamuła, B., Flejszar, R. (2019). Analysis of the accuracy of the reproduction of the solid model from the parametric surface in the module Reverse Engineering NX system. *Mechanik*, *7*, 468-470.

Celik, H.K., Rennie, A.E.W., Akinci, I. (2017). Reverse engineering approach for precise measurement of the physical attributes related to the geometric features of agricultural products. *Food Measure*, *11*(1), 75-84.

Costa, C., Antonucci, F., Pallottino, F., Aguzzi, J., Sun, D.W., Menesatti, P. (2011). Shape analysis of agricultural aroducts: A review of recent research advances and potential application to computer vision. *Food and Bioprocess Technology*, *4*(5), 673-692.

Dubravcik, M., Kender, S. (2012). Application of reverse engineering techniques in mechanics system services. *Procedia Engineering*, *48*, 96-104.

Gapinski, B., Wieczorowski, M., Marciniak-Podsadna, L., Dybala, B., Ziolkowski, G. (2014). Comparison of different method of measurement geometry using CMM, optical scanner and computed tomography 3D. *Procedia Engineering*, *69*, 255-262.

Kovacs, I., Varady, T., Salvi, P. (2015). Applying geometric constraints for perfecting CAD models in reverse engineering.*Graphical Models*, *82*, 44-57.

Pieróg, B.,Filipowicz, K., Pajor, M. (2020). Making copies of religious culture relics using reverse engineering. *Mechanik*, *4*, 16-19.

Sikorski, S., Duda, P., Dulęba, K., Wróbel, Z. (2016). Reverse engineering in modeling of hip replacement. *Mechanik*, *12*, 1912-1913.

Sokovic, M., Kopac, J. (2006). RE (reverse engineering) as necessary phase by rapid product development. *Journal of Materials Processing Technology*, *175(1-3)*, 398-403.

Vagovsky, J., Buransky, I., Gorog, A. (2015). Evaluation of measuring capability of the optical 3D scanner. *Procedia Engineering*, *100*, 1198-1206.

Wang, J., Gu, DX., Yu, ZY., Tan, CB., Zhou, LS. (2012). A framework for 3D model reconstruction in reverse engineering. *Computers & Industrial Engineering*, *63*(4), 1189-1200.

Ye, XZ., Liu, HZ., Chen, L., Chen, ZY., Pan, X., &Zhang, SY. (2008). Reverse innovative design - an integrated product design methodology. *Computer-Aided Design*, *40*(7), 812-827.

INŻYNIERIA ODWROTNA W MODELOWANIU PRODUKTÓW ROLNICZYCH

Streszczenie. Celem pracy było zastosowanie inżynierii odwrotnej do modelowania produktów pochodzenia biologicznego a w szególności korzenia buraka cukrowego. W procesie tworzenia modelu bryłowego wykorzystano odpowiednie narzędzia jakimi dysponuje środowisko do projektowania 3D. Pomocą w odwzorowaniu geometrii korzenia był trójwymiarowy skan buraka stanowiący przestrzenną chmurę punktów. Posłużyła ona do budowy siatki triangulacyjnej obejmującej punkty węzłowe trójkątów. W kolejnych krokach przedstawiono przebieg tworzenia modelu bryłowego za pomocą narzędzia *Splajn interpolacyjny*. Zwrócono uwagę na możliwości modyfikacji odtwarzania geometrii poprzez wprowadzanie kolejnych dodatkowych punktów do istniejącego *Splajnu interpolacyjnego* oraz zmiany położenia kątowego jak również odległości *Płaszczyzn konstrukcyjnych*. Wyznaczono wartości błędów odwzorowania geometrii w odniesieniu do modelu referencyjnego w zależności od wartości rozstawienia *Płaszczyzn konstrukcyjnych*. Przebiegi błędów mają charakter nieliniowy z logarytmiczną linią tredu – błąd pola powierzchni oraz z liniową linią tredu – błąd objętości. Na podstawie uzykanych efektów wykazano przydatność odtwarania geometrii i możliwość jej zastosowania do wspomagania badań wytrzymałościowych materiałów biologicznych ze szczególnym uwzględnieniem testów dynamicznych z wykorzystaniem całych korzeni.

Słowa kluczowe: inżynieria odwrotna, skan 3D, splajn interpolacyjny, odwzorowanie geometrii korzenia buraka cukrowego